Jyväskylän yliopiston julkaisuarkisto
Jyväskylä University Digital Archive

UNIVERSITY OF JYVÄSKYLÄ

This is an electronic reprint of the original article.
This reprint *may differ* from the original in pagination and typographic detail.

Author(s): Taylor, M.J.; Alharshan, G.A.; Cullen, David; Procter, M.G.; Lumley, N.M.; Grahn, Tuomas; Greenlees, Paul; Hauschild, Karl; Herzan, Andrej; Jakobsson, Ulrika; Jones, Peter; Julin, Rauno; Juutinen, Sakari; Ketelhut, Steffen; Leino, Matti; Lopez-Martens, Araceli; Nieminen, Päivi; Partanen, Jari; Peura, Pauli; Rahkila, Panu; Rinta-Antila, Sami; Ruotsalainen, Panu; Sandzelius, Mikael; Sarén, Jan; Scholey, Catherine; Sorri, Juha;

Title: Identification of isomeric states in the N=73 neutron-deficient nuclei 132Pr and 130La

Year: 2012

Version:

Please cite the original version:

Taylor, M.J., Alharshan, G.A., Cullen, D., Procter, M.G., Lumley, N.M., Grahn, T., Greenlees, P., Hauschild, K., Herzan, A., Jakobsson, U., Jones, P., Julin, R., Juutinen, S., Ketelhut, S., Leino, M., Lopez-Martens, A., Nieminen, P., Partanen, J., Peura, P., . . . Bai, Z.J. (2012). Identification of isomeric states in the N=73 neutron-deficient nuclei 132Pr and 130La. Physical Review C, 86(4), Article 044310. https://doi.org/10.1103/PhysRevC.86.044310

All material supplied via JYX is protected by copyright and other intellectual property rights, and duplication or sale of all or part of any of the repository collections is not permitted, except that material may be duplicated by you for your research use or educational purposes in electronic or print form. You must obtain permission for any other use. Electronic or print copies may not be offered, whether for sale or otherwise to anyone who is not an authorised user.

Identification of isomeric states in the $N = 73$ neutron-deficient nuclei ^{132}Pr and ^{130}La

M. J. Taylor,[1,*] G. A. Alharshan,[1] D. M. Cullen,[1] M. G. Procter,[1] N. M. Lumley,[1] T. Grahn,[2] P. T. Greenlees,[2] K. Hauschild,[2] A. Herzan,[2] U. Jakobsson,[2] P. Jones,[2] R. Julin,[2] S. Juutinen,[2] S. Ketelhut,[2] M. Leino,[2] A. Lopez-Martens,[2] P. Nieminen,[2] J. Partanen,[2] P. Peura,[2] P. Rahkila,[2] S. Rinta-Antila,[2] P. Ruotsalainen,[2] M. Sandzelius,[2] J. Sarén,[2] C. Scholey,[2] J. Sorri,[2] S. Stolze,[2] J. Uusitalo,[2] F. R. Xu,[3] and Z. J. Bai[3]

[1]*School of Physics & Astronomy, Schuster Laboratory, The University of Manchester, Manchester M13 9PL, United Kingdom*

[2]*Accelerator Laboratory, Department of Physics, University of Jyväskylä, Jyväskylä FIN-40014, Finland*

[3]*Department of Technical Physics and MOE Key Laboratory, Peking University, Beijing 100871, China*

(Received 13 August 2012; revised manuscript received 21 September 2012; published 8 October 2012)

Decays from isomeric states in the neutron-deficient $N = 73$ nuclei ^{132}Pr and ^{130}La have been observed for the first time. Half-lives of 486(70) ns and 2.46(4) μs were measured for two isomeric states in ^{132}Pr. The decay from the 486 ns (8^-) isomer has been interpreted as a hindered $E1$ transition from the bandhead state of the excited $\pi h_{11/2} \otimes \nu g_{7/2}$ configuration. The decay from the 2.5 μs (8^+) isomer is consistent with the Weisskopf estimate for a low-energy $E2$ transition. An analogous 0.74(3) μs decay from an (8^+) isomer in the neighboring isotone ^{130}La has also been observed which similarly can be explained if the transition has $E2$ character. The Weisskopf interpretation for the isomer hindrance is strengthened by the lack of evidence for shape or K isomerism due to the γ-soft shapes predicted by configuration-constrained potential-energy-surface calculations.

DOI: 10.1103/PhysRevC.86.044310 PACS number(s): 23.35.+g, 23.20.Lv, 21.10.Tg, 27.60.+j

I. INTRODUCTION

The discovery and measurement of isomeric nuclear states, with half-lives in excess of a nanosecond, are crucial in our understanding of nuclear structure. The long decay half-lives result from a significant difference between the wave functions of the initial and final states linking the decay. Most of the experimentally observed isomeric decays have been explained as either shape isomers, spin traps, or K isomers [1]. All three isomer types have been observed in $A \sim 120$–140 nuclei, which makes this area of the nuclear chart an ideal testing ground to investigate the underlying physics driving the isomerism. Spin-trap isomers are generally found in nuclei near closed shells where the reduced valence space limits the excited state density. K isomers occur in axially deformed nuclei when high-Ω orbitals are filled in the upper part of the shell. Shape isomers are often observed when a change from a highly deformed axially symmetric shape to a less deformed lower-energy configuration is needed to facilitate γ decay to the ground state.

The $Z = 59$ proton Fermi level for ^{132}Pr lies among the lower-Ω orbits of the $h_{11/2}$ shell that drive a prolate shape. However, the $N = 73$ neutron Fermi level lies among the higher-Ω orbits of the $h_{11/2}$ shell which favors an oblate shape. This competition results in soft nuclear shapes for nuclei in this region, which are susceptible to nonaxial deformations. Studies of ^{144}Ho [2,3], ^{142}Tb [2,4,5], ^{140}Eu [6], and ^{134,136}Pm [7,8] nuclei have unearthed isomers resulting from a change in nuclear shape linked by $E1$ γ-ray transitions. An interpretation of K isomerism was prohibited in these cases due to the γ softness associated with their shapes. It is uncertain whether these isomers truly are due to a change in nuclear shape or just due to the often hindered nature of the configuration changing $E1$ transitions. Systematic studies of $E1$ transitions have shown that decays between intrinsic states are often delayed compared to the single-particle Weisskopf or Nilsson estimates [9,10].

The first detailed γ-ray spectroscopic study of ^{132}Pr was performed by Shi *et al.* [11], who observed both signature components of two distinct rotational structures. One of the observed bands (band 1) was shown to be built on the near-prolate $\pi h_{11/2} \otimes \nu g_{7/2}$ configuration with the other (band 2) being built upon a $\pi h_{11/2} \otimes \nu h_{11/2}$ configuration with its associated triaxial shape. A similar scheme exists for the neighboring $N = 73$ isotone, ^{130}La, where two rotational structures have also been observed built upon $\pi h_{11/2} \otimes \nu g_{7/2}$ and $\pi h_{11/2} \otimes \nu h_{11/2}$ configurations [12]. In addition, Shi *et al.* also observed a decoupled band in ^{132}Pr, which was investigated further, along with a similar structure in ^{130}Pr, by Kondev *et al.* [13]. The work of Petrache *et al.* on ^{132}Pr [14] showed evidence for low-energy transitions depopulating the then assumed $\pi h_{11/2} \otimes \nu h_{11/2}$ bandhead state, which led to revised spin assignments for this band. It is important to note that the bandhead spin of 8 for the $\pi h_{11/2} \otimes \nu h_{11/2}$ band assigned by Shi *et al.* was based on systematics and the assumed perpendicular coupling of the spins of a low-Ω $h_{11/2}$ proton and a high-Ω $h_{11/2}$ neutron. A 47 keV $M1$ transition was reported, by Petrache *et al.*, to depopulate the proposed (7^-) bandhead of band 1; however, the intensity balance of the populated (6^-) level was not satisfied by the observed, low-intensity 40 and 98 keV decays that link the (6^-) state to the (6^+) and (5^+) states, respectively [14]. This suggested either the existence of other unobserved decay branches or a sizable lifetime for the (6^-) state.

The low-spin states in ^{132}Pr and ^{130}La have been investigated in β-decay studies (see Refs. [15] and [16], respectively). The β-decay work for ^{132}Pr suggested a ground-state spin of 2 from the observed feeding pattern and a positive parity was tentatively assigned. From a similar analysis for ^{130}La, a ground-state spin and parity of (3^+) was adopted. Links between the high-spin states, identified from in-beam γ-ray

*m.j.taylor@manchester.ac.uk

 ©2012 American Physical Society

spectroscopy studies, and the low-spin states, identified following β decay, are yet to be established for either nucleus. The motivation for this work was thus (i) to search for isomeric decays in ^{132}Pr and ^{130}La, (ii) attempt to link the low- and high-spin structures together, and (iii) to investigate further the reported intensity imbalance at the bottom of the $\pi h_{11/2} \otimes \nu g_{7/2}$ band in ^{132}Pr.

II. EXPERIMENTAL DETAILS

Excited states in ^{132}Pr and ^{130}La were populated via the fusion-evaporation reactions ^{98}Mo(^{40}Ar, $p5n$)^{132}Pr and ^{98}Mo(^{40}Ar, $\alpha p3n$)^{130}La, respectively. The K130 cyclotron, at the Accelerator Laboratory of the University of Jyväskylä, was used to accelerate an $^{40}Ar^{7+}$ beam to energies of 150, 158, and 165 MeV. The beam current averaged ∼4 pnA over an approximate running time of 82 h distributed 68%, 7%, and 25% for the 150, 158, and 165 MeV beam energies, respectively. All of the spectra shown in this article are created from the total data set unless otherwise stated. The accelerated ^{40}Ar nuclei were incident on an 800 μg/cm^2 ^{98}Mo target located at the center of the Jurogam-II γ-ray spectrometer [17], which recorded prompt γ rays following the reactions. For this work Jurogam-II comprised 39 Compton-suppressed germanium detectors, 15 Eurogam Phase-1 type detectors, and 24 clover detectors and had a total photopeak efficiency of ∼6% at 1332 keV.

Recoiling evaporation residues were separated from unreacted beam particles by the gas-filled recoil ion transport unit (RITU) [18,19] and were transported to the GREAT focal-plane spectrometer [20]. The mean recoil velocity of 2.5% v/c gives an average flight time through RITU of ∼0.5 μs. The GREAT spectrometer comprised a multi-wire proportional counter (MWPC), which resided in front of two double-sided silicon strip detectors (DSSD) [21], a planar Ge detector located behind the DSSDs, and a segmented clover detector orientated 90° above the planar detector. The separated evaporation residues were implanted into the DSSD. Conditions imposed on the time-of-flight (between the MWPC and the DSSD) and energy loss (in the MWPC) provided a method to distinguish scattered beam nuclei from reaction residues. Delayed γ rays from the decay of isomeric states and states populated following β decay were recorded by the planar and clover detectors. The planar detector had an estimated efficiency of ≈30% at 100 keV [20], making it ideally suited to the detection of low-energy γ-ray transitions from isomeric states. All events were time-stamped by a 100 MHz clock through the triggerless total data readout (TDR) acquisition system [22], allowing the correlations between prompt γ rays (detected at the target position) and delayed γ rays (detected at the focal plane of RITU) to be investigated.

III. RESULTS

The most intense delayed transitions observed in this experiment were those populated via β decay. Figure 1(a) shows delayed γ rays recorded by the focal plane planar Ge detector (within 40 μs of a recoil implantation) with the most intense β-delayed γ rays labeled with the parent nucleus [23–29]. The strongest evaporation channel was that of 4n (producing ^{134}Nd), which was also evident from the recoil-correlated prompt γ-ray data. As the β-decay half-lives for nuclei in this region range up to hundreds of milliseconds, decays from shorter-lived isomeric states can be emphasized by restricting the recoil-γ correlation time and subtracting a random-correlation background spectrum. To deduce an optimum recoil-γ correlation time a recoil-γ time versus γ-ray energy matrix was produced. For the time axis, the time difference between a γ-ray recorded in the planar Ge detector and the associated recoil implantation in the DSSD was used. The γ-ray energy, as recorded by the planar Ge detector, was used for the energy axis. Several decays whose intensities became negligible after 11 μs were clearly observed in the resulting matrix. Figure 1(b) shows a spectrum of delayed γ rays recorded by the planar Ge detector (within 11 μs of a recoil implantation) with a random-correlation background spectrum (produced from γ rays recorded up to 11 μs prior to the recoil implantation signal) subtracted. The β-delayed γ decays that dominate the spectrum in Fig. 1(a) are reduced in Fig. 1(b), leaving mostly decays from isomeric states.

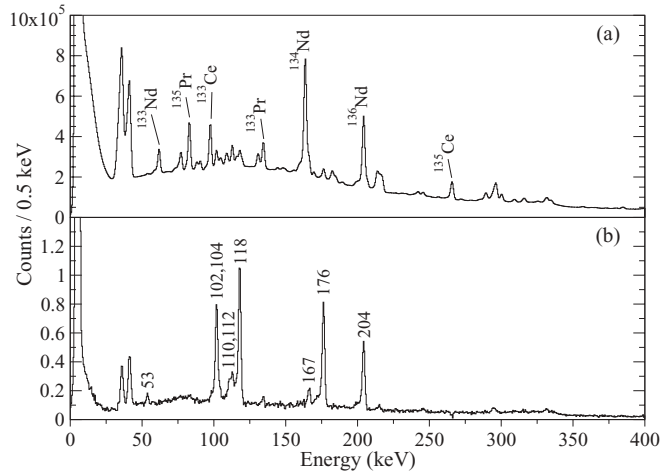

FIG. 1. Planar Ge detector spectra showing recoil-correlated delayed γ rays. (a) γ rays recorded within 40 μs of a recoil implantation. The majority of the transitions result from states populated by β decay, the most intense of which are labeled with the parent nucleus. (b) γ rays recorded within 11 μs of a recoil implantation. A random-correlation background spectrum of γ rays, recorded up to 11 μs prior to the recoil signal, was subtracted.

The intense peak in Fig. 1(b), at 176 keV, was identified as the decay from the known isomeric $9/2^-$ state in ^{133}Nd [30], produced via the 5n evaporation channel. A least-squares fit to the recoil-γ time distribution for this decay (Fig. 2) yielded a half-life of 291(4) ns, in excellent agreement with the current literature value of 301(18) ns [30]. This measurement confirmed both the energy and time calibrations for the DSSD and planar Ge detector.

A. ^{132}Pr

Other than the identified 176 keV decay in ^{133}Nd the most intense transitions in Fig. 1(b) occur at 118.0(1) and

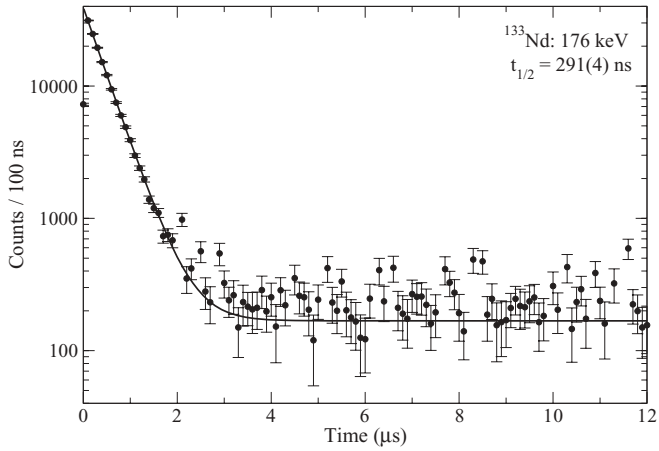

FIG. 2. Recoil-γ time distribution for the delayed 176 keV decay in ^{133}Nd. A least-squares fit yielded a half-life of 291(4) ns.

101.9(1) keV. A fit to the time distributions for these decays (Fig. 3) yielded half-lives of 2.48(5) and 2.43(7) μs, respectively. The similarity and consistency between the measured values suggests the decays lie below a common isomeric state, and a weighted mean of 2.46(4) μs is adopted as the state half-life. To identify the nucleus to which these decays belong a prompt-delayed (P-D) γ-γ coincidence matrix was produced with an optimum recoil-delayed γ correlation time of 9 μs and was background subtracted. A gate on the delayed 118 keV peak in this matrix produced a prompt γ-ray spectrum [Fig. 4(a)], whose peaks were all identified as known prompt transitions in ^{132}Pr [14]. Gating on prompt 283 keV γ rays and projecting onto the delayed axis of the P-D matrix showed the 118 and 102 keV delayed transitions [Fig. 4(b)]. Also observed were peaks at 36.0(2) and 41.0(2) keV, which are consistent with the Pr K_α and K_β x-ray lines with energies of 35.9 and 40.9 keV, respectively. For this experiment, the electronics for the planar Ge detector were adjusted to maximize γ-ray detection efficiency, which unfortunately reduced the detection efficiency for the lower-energy Pr x rays shown in Fig. 4(b). The x ray detection efficiency, relative to that at 100 keV, was

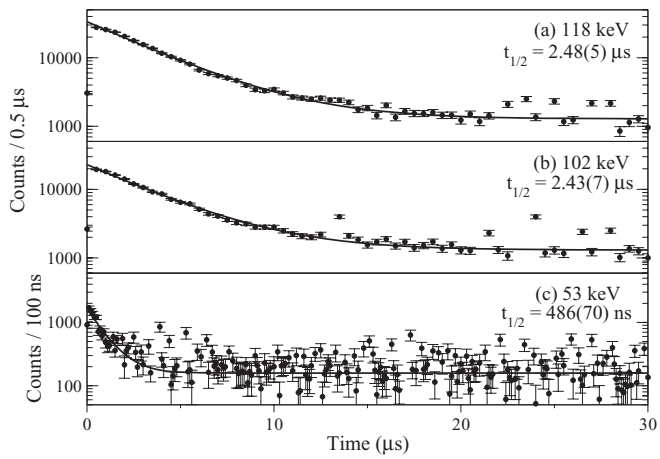

FIG. 3. Recoil-γ time distributions for the delayed (a) 118 keV, (b) 102 keV, and (c) 53 keV decays in ^{132}Pr along with least-squares fit curves.

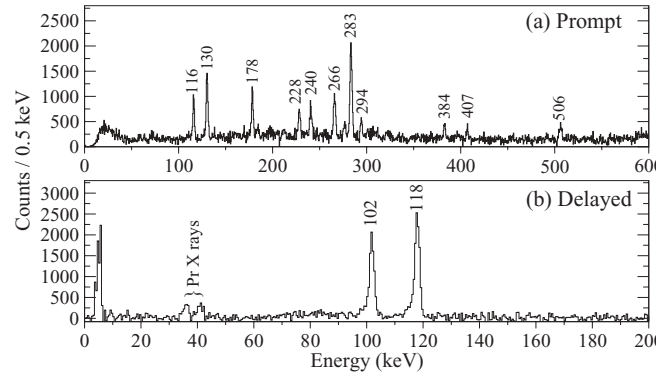

FIG. 4. Spectra produced from a prompt-delayed γ-γ coincidence matrix for ^{132}Pr. The matrix had an optimum recoil-delayed γ correlation time of 9 μs and was background subtracted. (a) Prompt γ rays that correlate with delayed 118 keV decays. (b) Delayed γ rays that correlate with prompt 283 keV decays.

measured to be approximately 9% and 22% for x rays at 36 and 41 keV, respectively.

A sum of prompt gates from the known positive-parity states [14], namely, the 283, 130, and 266 keV transitions in the P-D matrix, produced the delayed spectrum shown in Fig. 5(a). Similarly, gating on the prompt decays from the negative-parity states (116, 178, 228, and 277 keV transitions [14]) yielded Fig. 5(b), which contains a delayed γ-ray at 53.1(5) keV. A fit to the time distribution for this 53 keV transition [Fig. 3(c)] gave a half-life of 486(70) ns. The shorter measured half-life, relative to that observed in Figs. 3(a) and 3(b), indicates that the 53 keV γ ray depopulates a different isomeric state in ^{132}Pr, with higher excitation energy than the 2.5 μs state. The low-energy tails on the photopeaks in Figs. 1(b), 4(b), and 5 are due to incomplete charge collection in the planar Ge crystal.

A study of the low-spin structure of ^{132}Pr populated via the β decay of ^{132}Nd [15] revealed two parallel, noncoincident transitions with energies of 102.4(3) and 117.9(2) keV. A

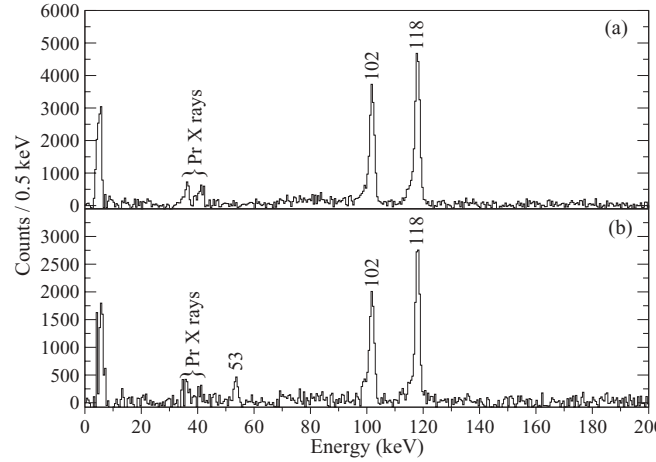

FIG. 5. Planar Ge spectra produced from a prompt-delayed γ-γ coincidence matrix with a 9 μs recoil-delayed γ correlation time (a) gated by the prompt 283, 130, and 266 keV transitions in ^{132}Pr and (b) gated by the prompt 116, 178, 228, and 277 keV transitions in ^{132}Pr.

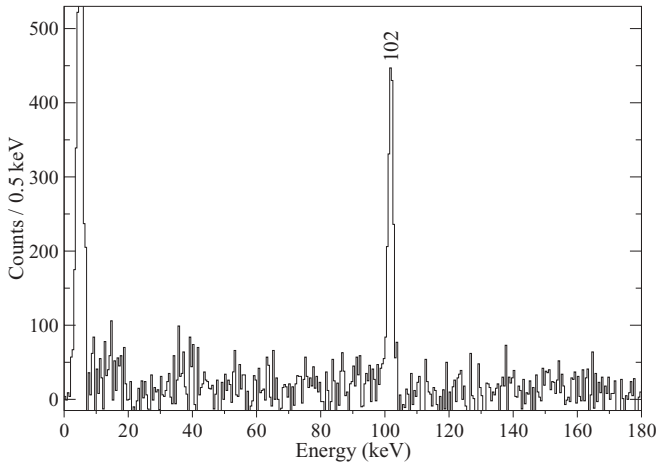

FIG. 6. Background-subtracted planar Ge detector spectrum showing delayed γ rays that were in coincidence (within 400 ns) with ^{132}Pr 118 keV decays recorded by the focal-plane clover detector. Both planar and clover signals correlated with a recoil implantation within 9 μs.

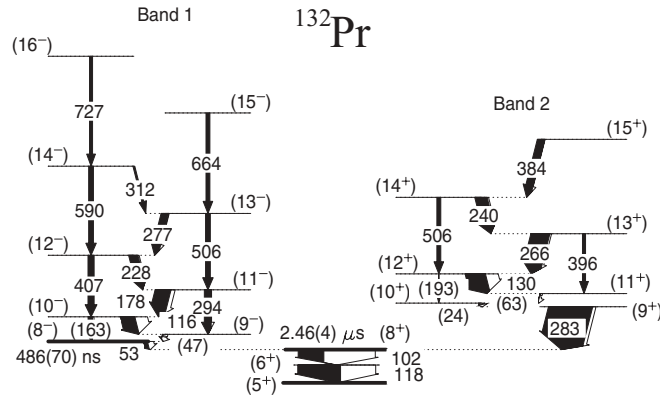

FIG. 7. Partial ^{132}Pr decay scheme produced in this work. The newly observed delayed γ rays at 53, 102, and 118 keV are tentatively positioned below the proposed (8^-) and (8^+) isomeric states. The weighted mean of the half-lives measured from the 102 and 118 decay time distributions is adopted as the half-life for the (8^+) state. Bracketed decays were reported in a previous study [14] but not observed in this work.

delayed-delayed (D-D) γ-γ coincidence matrix was produced from decays recorded in the focal plane clover and planar Ge detectors. The created D-D matrix contained planar Ge and clover detector signals that were recorded within 400 ns of each other, within 9 μs of a recoil implantation, and was background subtracted. This matrix was used to determine whether the 118 and 102 keV decays observed in this work were those established in Ref. [15]. The planar Ge spectrum created from a 118 keV clover detector gate is presented in Fig. 6. It is clear that the 102 keV decays are in coincidence with the 118 keV decays and thus cannot be the parallel transitions reported in the β-decay study [15]. The 118 and 102 keV decays must, therefore, be from an isomeric state and not from the states populated by β decay. Also, no other β-delayed transitions reported in Ref. [15] were observed.

The 102 keV transition in ^{132}Pr was also observed to overlap with a peak at ~104 keV, which did not correlate with the prompt ^{132}Pr decays shown in Fig. 4(a). A prompt γ-γ (PGG) coincidence matrix of γ rays that correlated with delayed ^{132}Pr 118 keV decays recorded within 9 μs of a recoil implantation was produced. Only the delayed 118 keV transition was used in the production of the matrix to ensure spectral cleanliness. Using this matrix, a partial decay scheme was developed (see Fig. 7). The proposed scheme incorporates the newly identified delayed transitions from this work. The measured energies, intensities, and tentatively assigned spins and parities of initial and final states are listed in Table I. The measured γ-ray intensities were efficiency corrected, using ^{152}Eu and ^{133}Ba calibration source data, with the prompt and delayed transitions normalized separately. The PGG coincidence matrix was used to confirm the ordering of the high-spin states reported in the literature [11,13,14] for ^{132}Pr; however, some transitions (shown in brackets in Fig. 7) reported in Ref. [14] were not observed in the present work. In particular, a 63 keV and an unobserved 24 keV transition were reported to link the 130 and 283 keV decays [14]. A 283 keV gated prompt spectrum produced from the 118 keV gated PGG matrix (Fig. 8) shows no evidence for a transition at 63 keV below the 130 keV decay. With the measured Jurogam-II

TABLE I. Intensities and γ-ray energies for ^{132}Pr measured in this work. The prompt and delayed intensities are normalized separately.

E_γ (keV)[a]	I_γ	$J_i^\pi \rightarrow J_f^\pi$
	Delayed γ rays[b]	
36.0(2)	103(7)	K_α
41.0(2)	44(2)	K_β
53.1(5)	10(1)	$(8^-) \rightarrow (8^+)$
101.9(1)	66(6)	$(8^+) \rightarrow (6^+)$
118.0(1)	100(11)	$(6^+) \rightarrow (5^+)$
	Prompt γ rays	
115.7(2)	33(1)	$(10^-) \rightarrow (9^-)$
129.9(2)	46(1)	$(12^+) \rightarrow (11^+)$
178.4(1)	36(3)	$(11^-) \rightarrow (10^-)$
228.1(1)	21(1)	$(12^-) \rightarrow (11^-)$
240.4(1)	28(1)	$(14^+) \rightarrow (13^+)$
265.6(1)	43(1)	$(13^+) \rightarrow (12^+)$
276.6(1)	17(1)	$(13^-) \rightarrow (12^-)$
283.1(1)	100(2)	$(9^+) \rightarrow (8^+)$
294.1(1)	16(1)	$(11^-) \rightarrow (9^-)$
312.4(1)	4(1)[c]	$(14^-) \rightarrow (13^-)$
383.5(1)	17(1)	$(15^+) \rightarrow (14^+)$
395.7(2)	7(1)	$(13^+) \rightarrow (11^+)$
407.0(1)	14(1)	$(12^-) \rightarrow (10^-)$
505.8(1)	11(1)[c]	$(13^-) \rightarrow (11^-)$
506.3(1)	9(1)[c]	$(14^+) \rightarrow (12^+)$
590.1(1)	11(1)[c]	$(14^-) \rightarrow (12^-)$
663.9(1)	9(1)[c]	$(15^-) \rightarrow (13^-)$
726.6(1)	7(1)[c]	$(16^-) \rightarrow (14^-)$

[a]Uncertainties on γ-ray energy are taken from a Gaussian fit.
[b]Intensities are taken from the spectrum shown in Fig. 5(b) and efficiency corrected.
[c]Intensities are determined from the γ-γ coincidence matrix and normalized.

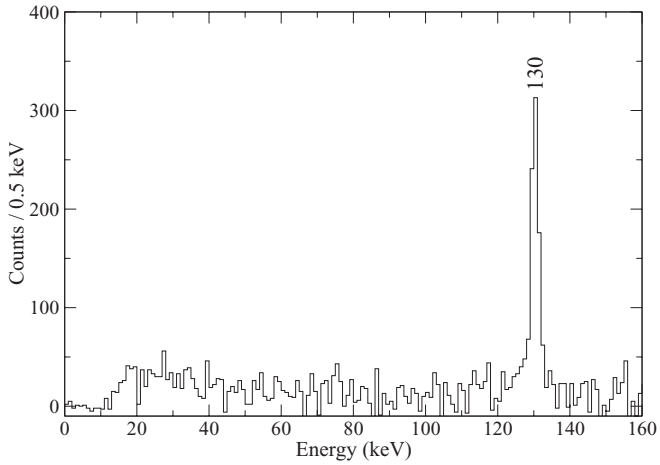

FIG. 8. The low-energy portion of a 283 keV-gated prompt spectrum produced from the 118 keV gated prompt γ-γ matrix which had a recoil-delayed γ time condition of 9 μs. The spectrum shows no evidence for correlated decays with energies below the 130 keV transition.

detection efficiency and intensities from Ref. [14], although highly converted, a 63 keV γ-ray peak would be expected to have just under 90 counts in the spectrum shown in Fig. 8, but this peak is clearly absent. The detection efficiency was determined from a fit to Ba/Eu source data; however, the γ-γ efficiency changes rapidly in this low-energy region. It is therefore possible that the efficiency is much lower than that determined from the fitting procedure and may be the reason why the 63 keV transition is absent in the present work. Likewise, a 24 keV $M1$ γ-ray transition would have around 2 counts in Fig. 8 and would, therefore, be far too weak to be observed in this work. The work of Kondev *et al.* [13] on ^{132}Pr also revealed no evidence for these transitions but the authors could not dismiss the possibility of there being a 63 keV transition based on feeding from an observed decoupled positive-parity band. The proposed decay scheme in this work (Fig. 7), therefore, shows the 130 keV decay depopulating the (12^+) state with the (9^+) state adopted as the bandhead (band 2). A systematic study of the positive-parity bands in all of the $N = 73$ and 75 isotones showed that the best consistent choice for the bandhead spin was $J = 9$ [31].

For the negative-parity band (band 1), a 47 keV transition and a weak 163 keV transition were reported in Ref. [14]. Although these decays were not observed in the present data, presumably due to limited statistics, they have also been included in Fig. 7. The correlations highlighted in Fig. 5 place the 53 keV decay below the 116 keV transition and above the 102 and 118 keV transitions. The parity-changing nature of the 53 keV decay (discussed later) restricts the possible multipolarities to $E1$, $M2$, $E3$, etc. The Weisskopf estimated half-life for an $M2$ decay is $\sim$1.8 ms and therefore it is most likely that the 53 keV decay is of $E1$ type. If band 1 had a bandhead-state spin of 7 then one may expect to observe a competing 155 keV [or 171 keV if the (8^+) state decayed via a 118 keV γ ray] decay feeding into the (6^+) state below the 2.5 μs isomer. The absence of any other competing γ rays observed in this work indicates a bandhead spin greater than 7 but less than 10. Weisskopf estimates for 155 keV $M2$ and $E3$ transitions yield half-lives of 8.5 μs and 0.5 s, respectively, in excess of that measured. Figure 7 shows the lowest feasible spin for the bandhead based on these arguments with the 53 keV decay out of the band being an unstretched $E1$ transition.

The prompt-delayed correlations for the 102 and 118 keV decays places them below band 2, being fed by the 283 keV transition. As only two delayed transitions have been observed to correlate with prompt transitions associated with band 2 it is unlikely that the observed decays feed into the $J = 2$ ground state [15] as this would require six units of spin to be accounted for. Also, the Weisskopf estimate for a 102 keV $M3$ transition yields a half-life in excess of 9 min for the depopulating state. A $t_{1/2} = 1.6$ min 5^+ isomer has been inferred in ^{132}Pr from the β-decay studies of Kortelahti *et al.* [32]. It is interesting to note that the neighboring isotope ^{134}Pr has a (2^-) ground state with an 11 min (6^-) isomer residing 68 keV above it. Decays from such a long-lived isomeric state fall outside of the sensitive range of the experimental setup used in this work; however, the existence of such a state is not ruled out by the data. It is, therefore, likely that the delayed 102 and 118 keV transitions feed into this predicted long-lived (5^+) isomer rather than the ground state. If this is the case then only three units of spin need to be accounted for by the two delayed transitions.

B. ^{130}La

Figure 1(b) shows a delayed transition at 110.2(2) keV whose time distribution has a half-life of 0.75(3) μs. This is shown in Fig. 9(a) along with the result of the least-squares fit used to extract the decay half-life. By reducing the recoil-γ correlation time to 2.5 μs, a spectrum of the prompt γ decays associated with the 110 keV delayed transition was produced from the resulting P-D matrix [see Fig. 10(a)]. The prompt decays have all been identified as those belonging to ^{130}La [12]. Gating on the most intense prompt peak in this spectrum at 137 keV yields the delayed spectrum shown in Fig. 10(b). The P-D correlation between the 137 and 110 keV decays is clear

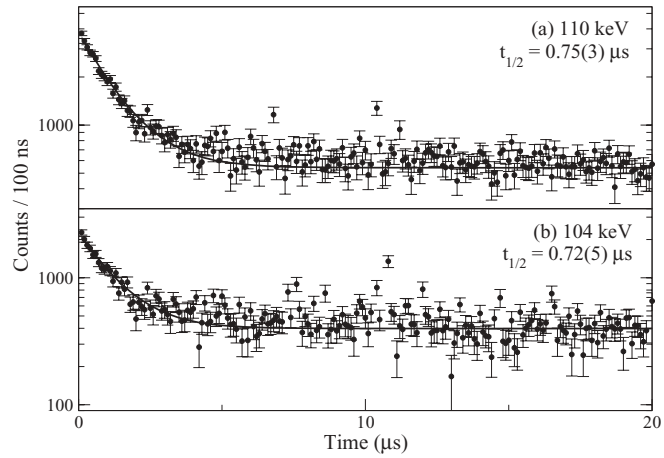

FIG. 9. Recoil-γ time distributions for the delayed (a) 110 keV and (b) 104 keV decays in ^{130}La along with least-squares fit curves.

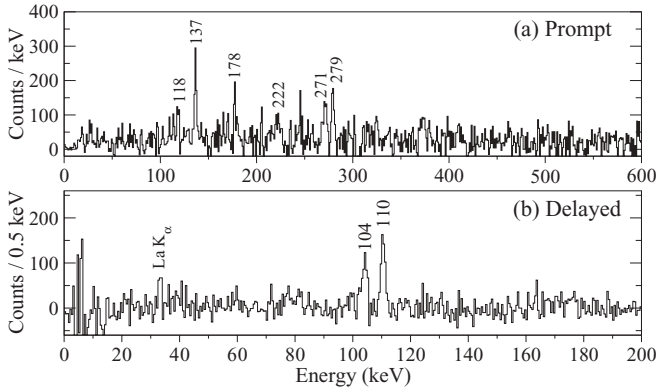

FIG. 10. Spectra produced from a prompt-delayed γ-γ coincidence matrix for ^{130}La. The matrix had an optimum recoil-delayed γ correlation time of 2.5 μs and was background subtracted. (a) Prompt γ rays that correlate with delayed 110 keV decays. (b) Delayed γ rays that correlate with prompt 137 keV decays.

but there is also a correlation with a peak at 103.9(2) keV. This delayed 104 keV peak, which forms a doublet with the delayed 102 keV decay in ^{132}Pr, was further identified as belonging to ^{130}La by gating on the 110 keV peak in a D-D matrix, the result of which can be seen in Fig. 11. A fit to the time distribution for the 104 keV decay, obtained from a narrow gate on a 0.1 keV/channel matrix (thus gating out the contribution from the 102 keV peak), yielded a half-life of 0.72(5) μs. This suggests that the 104 and 110 keV decays lie below a common isomeric state and a weighted mean of 0.74(3) μs is adopted as the state half-life. Two transitions at 103.9(2) and 110.4(2) keV have been observed following the EC/β^+ decay of ^{130}Ce [16] with the 110 keV transition shown to be isomeric with a half-life of 17(5) ns. The proposed low-spin decay scheme in Ref. [16], however, showed no feeding pattern between the two decays. As was the case for the 102 and 118 keV delayed transitions in ^{132}Pr, the data suggest that not only are the 104

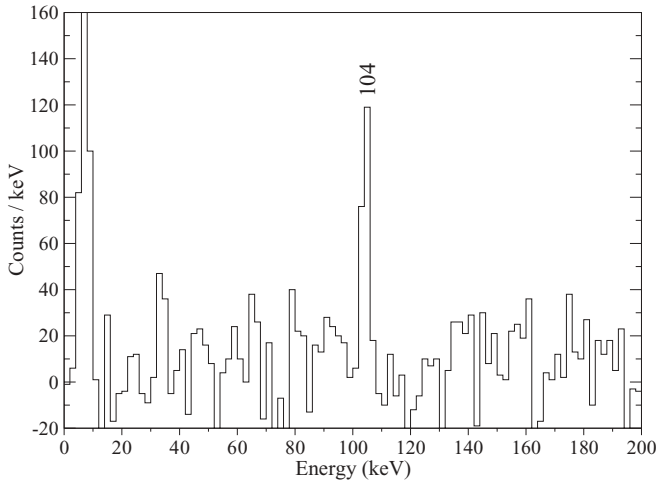

FIG. 11. Background-subtracted planar Ge detector spectrum showing delayed γ rays that were in coincidence (within 400 ns) with ^{130}La 110 keV decays recorded by the focal-plane clover detector. Both planar and clover signals correlated with a recoil implantation within 2.5 μs.

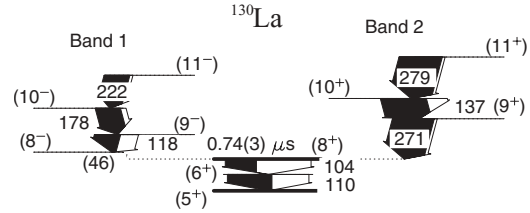

FIG. 12. Partial ^{130}La decay scheme produced in this work. The newly observed delayed γ rays at 104 and 110 keV are tentatively positioned below the proposed (8$^+$) isomeric state. The weighted mean of the half-lives measured from the 104 and 110 decay time distributions is adopted as the half-life for the (8$^+$) state. The 46 keV decay was reported in a previous study [12] but not observed in this work.

and 110 keV transitions in ^{130}La linked via an intermediate state but that they are not the 104 and 110 keV transitions observed following the β decay of ^{130}Ce.

Figure 12 shows a partial decay scheme for ^{130}La developed using Fig. 10(a) and Ref. [12]. Due to a lack of statistics, tagged prompt-γ-γ coincidences could not be used to independently confirm the prompt level ordering; therefore, all assignments are based on those reported in Ref. [12]. Table II summarizes the transitions in ^{130}La observed in this work. The 46 keV decay out of band 1, which was reported in Ref. [12], was not observed in this work. If one assumes this transition is analogous to the 53 keV isomeric decay in ^{132}Pr then the nonobservation of this transition in Fig. 10(b) could be explained by the limited statistics resulting from the lower production cross section for ^{130}La.

C. Other isomeric decays

The remaining γ rays labeled in Fig. 1(b) have all been identified as decays from known isomeric states in other reaction products. The 112 keV peak is the known $M2$ decay from the 105(10) μs 11/2$^{(-)}$ isomer in ^{135}Pr [33]. There are

TABLE II. Intensities and γ-ray energies for ^{130}La measured in this work. The prompt and delayed intensities are normalized separately. The tentative initial and final spins are based on those reported in Ref. [12].

E_γ (keV)[a]	I_γ	$J_i^\pi \rightarrow J_f^\pi$
	Delayed γ rays[b]	
103.9(2)	70(7)	(8$^+$) → (6$^+$)
110.2(2)	100(11)	(6$^+$) → (5$^+$)
	Prompt γ rays	
118.2(1)	57(3)	(9$^-$) → (8$^-$)
177.6(1)	55(3)	(10$^-$) → (9$^-$)
222.0(2)	56(4)	(11$^-$) → (10$^-$)
271.3(1)	91(5)	(9$^+$) → (8$^+$)
136.6(1)	100(5)	(10$^+$) → (9$^+$)
279.3(1)	94(5)	(11$^+$) → (10$^+$)

[a]Uncertainties on γ-ray energy are taken from a Gaussian fit.
[b]Intensities are taken from the spectrum shown in Fig. 10(b) and efficiency corrected.

TABLE III. Energy eigenvalues (in MeV) from configuration-constrained calculations for possible configurations with orbitals close to the Fermi surface.

$\nu\backslash\pi$	$3/2^+[411]$	$3/2^-[541]$	$1/2^-[550]$
$9/2^-[514]$	0.131	0.045	0.047
$7/2^+[404]$	0.088	0.000	0.007

subsequent decays at 204 and 41 keV which link the $11/2^{(-)}$ isomeric state with the $3/2^{(+)}$ ground state in ^{135}Pr. These transitions are also present in Fig. 1(b). The peak at 167 keV is the decay from the known 410(30) μs $(8)^-$ isomer in ^{134}Nd [34]. These assignments have been confirmed using P-D and D-D analyses where appropriate.

IV. DISCUSSION

A. ^{132}Pr

Nuclei in the $A \sim 130$ region are known to exhibit prolate [35,36] and triaxial [37] deformation with varying degrees of γ softness. Cranked shell model (CSM) calculations performed by Shi *et al.*, the details of which can be found in Ref. [11], showed that for ^{132}Pr the $\pi h_{11/2} \otimes \nu g_{7/2}$ configuration stabilizes at a near prolate shape and the $\pi h_{11/2} \otimes \nu h_{11/2}$ configuration at a near triaxial shape with $\gamma \sim -10^\circ$. To ascertain whether the long measured half-life for the $(8^-) \rightarrow (8^+)$ transition, via the newly observed 53 keV γ decay, results from a change in nuclear shape, configuration-constrained calculations for the low-lying states of ^{132}Pr were performed. Table III shows the resulting energy eigenvalues, within 200 keV of the calculated ground state, for configurations involving orbitals near the Fermi surface. It is clear from the values in Table III that the ground state of ^{132}Pr could result from a number of possible configurations and that the ground-state wave function is likely to be of a severely mixed nature.

Due to the close proximity of a number of orbitals near the Fermi surface, predicting the simplest of quantities, such as the ground-state parity, is not trivial. The calculations show that a number of positive- and negative-parity configurations lie within 140 keV of each other. The currently adopted spin and parity for the ground state is $2^{(+)}$ based on β-decay studies [15] and comparison with neighboring isotopes, although the parity assignment is tentative. Shi *et al.* proposed a dominant $\pi 3/2^-[541] \otimes \nu 7/2^+[404]$ configuration for the negative-parity band and either a $\pi 3/2^-[541] \otimes \nu 7/2^-[523]$ or a $\pi 3/2^-[541] \otimes \nu 9/2^-[514]$ configuration for the positive-parity band based on a quadrupole deformation characterized by $\beta = 0.2$. In the present work, potential-energy-surface (PES) calculations were performed and the surface plots for the three low-lying configurations, postulated by the experimental work of Shi *et al.*, are shown in Fig. 13. The plots show no evidence for a change in shape between the negative-parity and positive-parity configurations that could lead to isomerism. A ground-state configuration of $\pi 3/2^-[541] \otimes \nu 7/2^+[404]$, as predicted by the calculations, results in $\beta_2 = 0.24$ (in agreement with that suggested by Shi *et al.*) but the apparent γ softness of the resulting shapes argues against the (8^-) state being a K isomer.

If one assumes a parity-changing $E1$ nature for the 53 keV transition in ^{132}Pr, the Weisskopf single-particle transition probability implies a half-life of 1.7 ps, which cannot account for the measured half-life of 486(70) ns. The large hindrance corresponds to a reduced transition probability of

$$S = \frac{t_{1/2}(\text{Weisskopf})}{t_{1/2}(\text{experiment})} = 1.48 \times 10^{-6} \qquad (1)$$

if one uses the Weisskopf single-particle estimate corrected for internal conversion ($\alpha = 1.37$ [38]). This reduced transition probability is, however, consistent with that expected, $\sim 10^{-7}$, based on a systematic study of $E1$ transitions in this region [10]. For example, the 37 keV $(8^+) \rightarrow (7^-)$, 300 ns $E1$ transition in ^{140}Eu has a reduced transition probability $S = 7.6(8) \times 10^{-6}$.

By using the Weisskopf single-particle estimate, corrected for internal conversion, for a 102 keV $E2$ transition the decay would proceed with $t_{1/2} = 440$ ns, resulting in a transition hindrance factor of $\sim$5. The microsecond half-life of the (8^+) state can, therefore, be understood if the depopulating transition has $E2$ character. The consistency, within their associated errors, between the half-lives, determined from the recoil-γ time distributions, could be an indication that the lifetime of the intermediate (6^+) state is considerably less than that of the (8^+) state. This would suggest that the 118 keV decay is an $M1$ transition with a Weisskopf estimated half-life of 8 ps. The measured microsecond half-life could also be explained if the (8^+) state was depopulated by a 118 keV $E2$ transition; however, the ordering in Fig. 7 is based on the lower hindrance achieved with a 102 keV $E2$ decay. The $E2$ and $M1$ assignment is corroborated further by the intensity of the observed Pr x rays. Although the associated x-ray intensities for individual γ-ray transitions could not be established, a comparison between the total x-ray and γ-ray intensities for the sum of the 102 and 118 keV decays could be made. The x-ray and γ-ray intensities taken from Fig. 5(a) are consistent with those expected for the $E2$ and $M1$ assignments for the 102 and 118 keV decays, respectively, based on K conversion coefficients calculated using Band-raman Internal conversion coefficients (BrIcc) [38]. A similar analysis was performed using the spectrum shown in Fig. 5(b), whose normalized intensities are shown in Table I. Assuming $E1$ for the 53 keV transition and $E2$ and $M1$ for the 102 and 118 keV decays, respectively, the summed x-ray intensity is consistent with the summed γ-ray intensity using calculated conversion coefficients, thus adding further support to the $E1$ assignment for the 53 keV transition.

B. ^{130}La

The data for the $N = 73$ isotone ^{130}La follow a similar pattern to that of ^{132}Pr, which is reflected in the correlation spectra shown in Fig. 10 and in the proposed decay scheme of Fig. 12. Unfortunately, the lower production cross section for ^{130}La, relative to that of ^{132}Pr, meant that a γ-γ coincidence analysis could not be performed to confirm the ordering

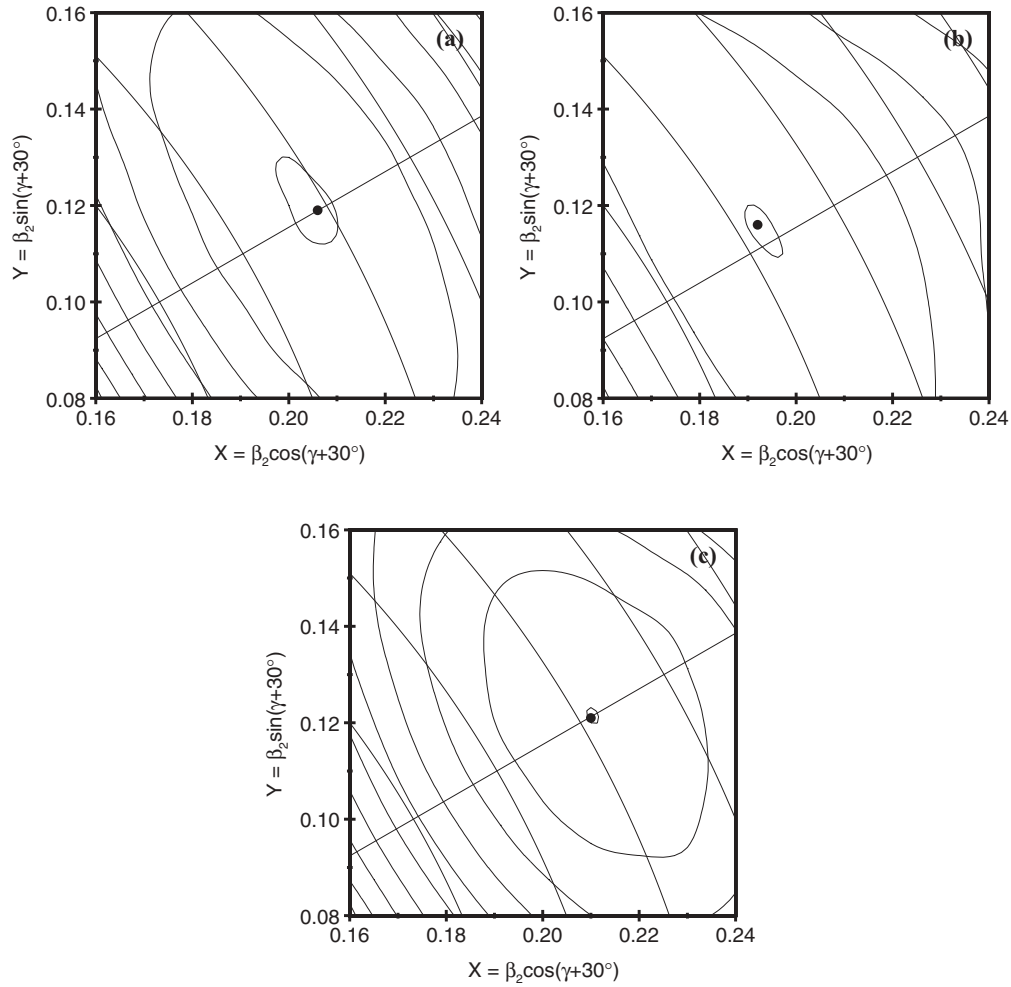

FIG. 13. The results of potential-energy-surface calculations for the proposed (a) $\pi 3/2^-[541] \otimes \nu 7/2^+[404]$ negative-parity band configuration along with two possible configurations (b) $\pi 3/2^-[541] \otimes \nu 7/2^-[523]$ and (c) $\pi 3/2^-[541] \otimes \nu 9/2^-[514]$ for the positive-parity band in ^{132}Pr.

of the prompt decays. The ordering in Fig. 12 is therefore based on measured intensities and the decay scheme reported in Ref. [12]. Unlike in ^{132}Pr, however, there was no clear evidence for an isomeric negative-parity bandhead state. This could be due to a lack of statistics arising from the lower production cross section for ^{130}La relative to that for ^{132}Pr. For the 104 and 110 keV decays, the calculated half-lives based on Weisskopf single-particle transition probabilities and corrected for internal conversion are 0.44 and 0.38 μs, respectively. Similarly to ^{132}Pr, the isomeric nature of the (8^+) state in ^{130}La can also be understood if the depopulating γ ray is of $E2$ type. The ordering of the 104 and 110 keV decays replicates that of the analogous transitions in ^{132}Pr; however, the isomeric nature of the (8^+) state can also be understood if the ordering is reversed.

V. SUMMARY

Decays from two new isomeric states have been observed in the $N = 73$ nucleus ^{132}Pr. A 53 keV, 486(70) ns decay has been assigned, through prompt-delayed γ-ray coincidences, as the decay out of the $\pi h_{11/2} \otimes \nu g_{7/2}$ negative-parity bandhead into an (8^+) isomeric state possibly built upon a $\pi h_{11/2} \otimes \nu h_{11/2}$ configuration. The 53 keV transition has been interpreted as a hindered $E1$ transition, whose reduced transition probability is consistent with those for similar $E1$ transitions observed in this region of the nuclear chart. Potential-energy-surface calculations showed no evidence for a change in shape between these configurations, ruling out shape isomerism as the cause of the long measured half-life. The calculations also revealed a large degree of γ softness for these configurations, which argues against K isomerism. Decays (at 102 and 118 keV) below the 2.46(4) μs (8^+) isomer have also been observed, the half-life of which can be explained through Weisskopf single-particle transition probabilities if either of the two decays have $E2$ character. Prompt-delayed correlations show this 2.5 μs isomeric state to reside below an excited $\pi h_{11/2} \otimes \nu h_{11/2}$ band with the observed decays believed to feed into a predicted $t_{1/2} = 1.6$ min 5^+ isomer. Analogous decays at 104 and 110 keV have been observed in neighboring ^{130}La; however, no isomeric decays out of the negative-parity bandhead were observed presumably due to insufficient statistics. In both nuclei, prompt-delayed γ-γ analysis did not provide any links between the low-spin states populated in β decay and

the high-spin states identified in in-beam γ-ray spectroscopy studies.

ACKNOWLEDGMENTS

This work has been supported by the EU 7th Framework Programme, "Integrating Activities—Transnational Access," Project No. 262010 (ENSAR), and by the Academy of Finland under the Finnish Centre of Excellence Programme 2006–2011 (Nuclear and Accelerator Based Physics Programme at JYFL). The authors acknowledge the support of GAMMAPOOL for the loan of the JUROGAM detectors. MGP, DMC, and MJT acknowledge the support of the STFC through Contract No. ST/G008787/1. PTG acknowledges the support of the Academy of Finland through Contract No. 119290. GAA is supported by the Princess Nora bint Abdulrahman University and the Ministry of Higher Education of Saudi Arabia.

[1] P. Walker and G. Dracoulis, Nature (London) **399**, 35 (1999).
[2] C. Scholey *et al.*, Phys. Rev. C **63**, 034321 (2001).
[3] P. J. R. Mason *et al.*, Phys. Rev. C **81**, 024302 (2010).
[4] P. J. R. Mason *et al.*, Phys. Rev. C **79**, 024318 (2009).
[5] M. N. Tantawy *et al.*, Phys. Rev. C **73**, 024316 (2006).
[6] D. M. Cullen *et al.*, Phys. Rev. C **66**, 034308 (2002).
[7] D. M. Cullen *et al.*, Phys. Rev. C **80**, 024303 (2009).
[8] S. V. Rigby *et al.*, Phys. Rev. C **78**, 034304 (2008).
[9] K. E. G. Löbner, Phys. Lett. B **26**, 369 (1968).
[10] K. Löbner, Nucl. Phys. A **80**, 505 (1966).
[11] S. Shi, C. W. Beausang, D. B. Fossan, R. Ma, E. S. Paul, N. Xu, and A. J. Kreiner, Phys. Rev. C **37**, 1478 (1988).
[12] M. J. Godfrey, Y. He, I. Jenkins, A. Kirwan, P. J. Nolan, D. J. Thornley, S. M. Mullins, and R. Wadsworth, J. Phys. G **15**, 487 (1989).
[13] F. G. Kondev *et al.*, Phys. Rev. C **59**, 3076 (1999).
[14] C. M. Petrache, S. Brant, D. Bazzacco, G. Falconi, E. Farnea, S. Lunardi, V. Paar, Z. Podolyák, R. Venturelli, and D. Vretenar, Nucl. Phys. A **635**, 361 (1998).
[15] D. Bucurescu *et al.*, Nucl. Phys. A **587**, 475 (1995).
[16] S. Xu *et al.*, Z. Phys. A **356**, 35 (1996).
[17] P. T. Greenlees *et al.*, AIP Conf. Ser. **764**, 237 (2005).
[18] M. Leino *et al.*, Nucl. Instrum. Methods Phys. Res., Sect. B **99**, 653 (1995).
[19] J. Sarén, J. Uusitalo, M. Leino, and J. Sorri, Nucl. Instrum. Methods Phys. Res., Sect. A **654**, 508 (2011).
[20] R. D. Page *et al.*, Nucl. Instrum. Methods Phys. Res., Sect. B **204**, 634 (2003).
[21] P. T. Greenlees *et al.*, Eur. Phys. J. A Suppl. **25**, 599 (2005).
[22] I. Lazarus *et al.*, IEEE Trans. Nucl. Sci. **48**, 567 (2001).
[23] J. B. Breitenbach, J. L. Wood, M. Jarrio, R. A. Braga, H. K. Carter, J. Kormicki, and P. B. Semmes, Nucl. Phys. A **595**, 481 (1995).
[24] R. Arlt *et al.*, Bull. Acad. Sci. USSR, Phys. Ser. **36**, 673 (1973).
[25] E. A. Henry and R. A. Meyer, Phys. Rev. C **18**, 1814 (1978).
[26] M. S. Rapaport, D. Bucurescu, C. F. Liang, and P. Paris, Phys. Rev. C **42**, 1959 (1990).
[27] A. A. Sonzogni, Nucl. Data Sheets **103**, 1 (2004).
[28] A. A. Abdumalikov, A. Zhumamuratov, T. A. Islamov, V. U. Kalinnikov, V. V. Kuznetsov, L. Z. Sik, N. A. Lebedev, and N. Z. Marupov, Tech. Rep. JINR-P6-81-489, 1981.
[29] A. Abdurazakov, T. Vylov, M. Enikova, Z. Zhelev, T. Islamov, N. Lebedev, G. Kononenko, and A. Ioushkevitch, Bulg. J. Phys. **8**, 556 (1981).
[30] Y. Khazov, A. Rodionov, and F. G. Kondev, Nucl. Data Sheets **112**, 855 (2011).
[31] Y. Liu, J. Lu, Y. Ma, S. Zhou, and H. Zheng, Phys. Rev. C **54**, 719 (1996).
[32] M. O. Kortelahti, B. D. Kern, R. A. Braga, R. W. Fink, I. C. Girit, and R. L. Mlekodaj, Phys. Rev. C **42**, 1267 (1990).
[33] B. Singh, A. A. Rodionov, and Y. L. Khazov, Nucl. Data Sheets **109**, 517 (2008).
[34] A. A. Sonzogni, Nucl. Data Sheets **103**, 1 (2004).
[35] L. Hildingsson, C. W. Beausang, D. B. Fossan, and W. F. Piel Jr., Phys. Rev. C **33**, 2200 (1986).
[36] C. W. Beausang, L. Hildingsson, E. S. Paul, W. F. Piel Jr., P. K. Weng, N. Xu, and D. B. Fossan, Phys. Rev. C **36**, 602 (1987).
[37] R. Aryaeinejad, D. J. G. Love, A. H. Nelson, P. J. Nolan, P. J. Smith, D. M. Todd, and P. J. Twin, J. Phys. G **10**, 955 (1984).
[38] T. Kibédi, T. W. Burrows, M. B. Trzhaskovskaya, P. M. Davidson, and C. W. Nestor, Nucl. Instrum. Methods Phys. Res., Sect. A **589**, 202 (2008).